Ultrastructure of the Epidermal Cell Wall and Cuticle of Tomato Fruit (*Solanum lycopersicum* L.) during Development[1][OPEN]

Patricia Segado, Eva Domínguez, and Antonio Heredia*

Instituto de Hortofruticultura Subtropical y Mediterránea La Mayora, Universidad de Málaga - Consejo Superior de Investigaciones Científicas, Departamento de Biología Molecular y Bioquímica, Universidad de Málaga, E-29071 Málaga, Spain (P.S., A.H.); and Departamento de Mejora Genética y Biotecnología, Estación Experimental La Mayora, Algarrobo-Costa, E-29750 Málaga, Spain. (E.D.)

ORCID ID: 0000-0002-3328-1115 (A.H.).

The epidermis plays a pivotal role in plant development and interaction with the environment. However, it is still poorly understood, especially its outer epidermal wall: a singular wall covered by a cuticle. Changes in the cuticle and cell wall structures are important to fully understand their functions. In this work, an ultrastructure and immunocytochemical approach was taken to identify changes in the cuticle and the main components of the epidermal cell wall during tomato fruit development. A thin and uniform procuticle was already present before fruit set. During cell division, the inner side of the procuticle showed a globular structure with vesicle-like particles in the cell wall close to the cuticle. Transition between cell division and elongation was accompanied by a dramatic increase in cuticle thickness, which represented more than half of the outer epidermal wall, and the lamellate arrangement of the non-cutinized cell wall. Changes in this non-cutinized outer wall during development showed specific features not shared with other cell walls. The coordinated nature of the changes observed in the cuticle and the epidermal cell wall indicate a deep interaction between these two supramolecular structures. Hence, the cuticle should be interpreted within the context of the outer epidermal wall.

The epidermis is the tissue that covers all plant organs. It is composed of thick-walled cells that are strongly adhered to each other and display specific mechanical properties that confer the necessary strength to support plant integrity and control plant growth (Kutschera and Niklas, 2007; Savaldi-Goldstein et al., 2007; Javelle et al., 2011). In addition to differences in cell wall thickness between the epidermis and the rest of inner tissues, there is also asymmetry within epidermal cell walls (Glover, 2000). The outer epidermal wall (OEW), being the structure that bears most of the stress exerted by growing internal tissues, is considerably thicker than the inner periclinal and anticlinal walls (Glover, 2000; Kutschera, 2008). This asymmetry is further reinforced by the deposition of a lipid-rich and highly hydrophobic cuticle layer.

The plant cuticle is a protective layer that covers the outer wall of the aerial parts of higher plants. It constitutes the primary barrier between the atmosphere and the plant, thus serving different protective functions (Heredia, 2003). In this sense, the cuticle prevents massive water loss, regulates gas exchange, protects against mechanical injury and pathogen invasion, filters potentially damaging UV light, and generates a microenvironment suitable for certain organisms (Holloway, 1982; Riederer and Müller, 2006; Domínguez et al., 2011; Yeats and Rose, 2013). In the last years, a role for the cuticle in postharvest fruit quality has been manifested (Becker and Knoche, 2012; Lara et al., 2014; Martin and Rose, 2014). Most of these functions have been demonstrated for isolated cuticles; however, it should not be forgotten that the epidermis contributes to these properties in planta.

The cuticle has a complex and heterogeneous nature. It is composed of a fraction of soluble waxes (Samuels et al., 2008), mainly devoted to reducing water transport, deposited on and in an insoluble matrix of cutin, which constitutes the main component of the cuticle. A minor phenolic fraction is also present in the cutin matrix (Hunt and Baker, 1980). Cutin forms an amorphous and viscoelastic framework based on the interesterification of C_{16} and C_{18} polyhydroxyalkanoic acids (Heredia, 2003; Domínguez et al., 2011). The significant progress made toward understanding cutin chemical composition and its monomer biosynthesis (Heredia,

[1] This work was partially supported by grant no. AGL2012-32613 of the Plan Nacional de I+D, Ministry of Education and Science, Spain.

* Address correspondence to heredia@uma.es.

The author responsible for distribution of materials integral to the findings presented in this article in accordance with the policy described in the Instructions for Authors (www.plantphysiol.org) is: Antonio Heredia (heredia@uma.es).

P.S. carried out the experiments; and E.D. and A.H. interpreted the data and wrote the manuscript.

[OPEN] Articles can be viewed without a subscription.

www.plantphysiol.org/cgi/doi/10.1104/pp.15.01725

 © 2016 American Society of Plant Biologists. All Rights Reserved.

2003; Pollard et al., 2008; Beisson et al., 2012) has recently been accompanied by a partial description of the mechanism of transport and further synthesis of cutin (Heredia-Guerrero et al., 2008; Girard et al., 2012; Yeats et al., 2012; Domínguez et al., 2015).

The cuticle membrane lies over and merges into the outer wall of epidermal cells (Martin and Juniper, 1970). Thus, a fraction of cell wall polysaccharides is embedded in the cuticle and can be regarded as a cuticle component. This polysaccharide fraction present in the isolated cuticle is variable among species and developmental stages, depending on the degree of merging between the cutin matrix and the cell wall. Hence, the cuticle can be considered a fine modification of the epidermal cell wall or an integral part of it, since it is already present during embryogenesis (Javelle et al., 2011). Again, due to the deep association between the cuticle and the cell wall, they both have overlapping properties and functions (Thompson, 2001).

A lot of work has been carried out on the fine structure of the cuticle and cell wall. Jeffree (2006) compiled and analyzed the state-of-the-art data on cuticle fine structure for a large number of plant species. Various cuticle morphological and structural types, from lamellate and relatively ordered structures to reticulate and mainly amorphous ones, have been observed in different plant species (Jeffree, 2006). Moreover, changes in cuticle morphology and structure can be displayed during plant development (Riederer and Schönherr, 1988). This complex ultrastructural scenario needs to be integrated with our still incomplete knowledge on the synthesis and assembly of cuticle components, mainly cutin, and their interactions with an evolving cell wall. Cell wall ultrastructure has usually been analyzed with antibodies against different polysaccharide components, and mostly performed to study cell wall changes during fruit ripening. However, the structure and function of growing cell walls and their cuticle membranes is still not clear (Fry, 2004; Jeffree, 2006). In order to gather knowledge on the OEW functions, it is important to investigate the modifications and distribution of their components as well as their dynamic changes. Despite the significant role of the epidermis and cuticle on plant growth and interaction with the environment, there is scarce literature on their structural and morphological changes during plant development.

Tomato fruit has been extensively analyzed at the cell wall and cuticle levels due to its economic importance. Significant information on the biophysical (Bargel et al., 2006; Domínguez et al., 2011), physiological (Baker et al., 1982; Domínguez et al., 2008), and biochemical (Lunn et al., 2013) properties of the cuticle has been gathered over the years as well as on the physiological changes occurring during fruit growth and ripening (Seymour et al., 2013). This work studies the morphological and structural modifications of epidermal cells and cuticle during tomato fruit development. A study of this nature is also necessary for a better understanding of the formation of the biopolymer cutin. In this sense, in this work we draw a detailed ultrastructural scenario of the genesis and further development of tomato fruit cuticle. Thus, the aim of this research is 2-fold: to describe changes of fine structure of cuticle and epidermal cell wall in the course of tomato fruit development, and to correlate the already existing information on cuticle chemical composition and biophysical characteristics with its fine structure.

RESULTS

Fig. 1 shows changes in the number of epidermal cells per surface unit during fruit growth and development. The period of cell division corresponded to approximately the first 10 days after anthesis (daa) while from 11 daa, cell expansion became prominent. The number of cells per surface area did not remain constant during the cell division period but decreased once fruit was set and started its growth (2 daa) and then remained constant until 8 daa. Two consecutive and significant drops in the number of cells were observed at 9 and 11 daa. From 11 daa, the number of epidermal cells per surface area slowly decreased until it reached a minimum at red ripe. A transition period between cell division and cell enlargement was observed at 9 to 10 daa, where a combination of cell division and cell expansion was observed.

Epidermal Fine Structure at Early Stages of Development

Fig. 2 shows transverse sections of Cascada fruit tissue during the first 6 d of organ growth. At anthesis, no tissue differentiation was observed, with all cells showing irregular shapes and sizes. However, the outer wall of protodermal cells, still not differentiated as epidermis, already displayed a higher thickness in comparison to the radial or inner walls (Fig. 2A). These protodermal cells were not arranged in the same plane, but some cells protruded. At 2 daa, fruit surface began

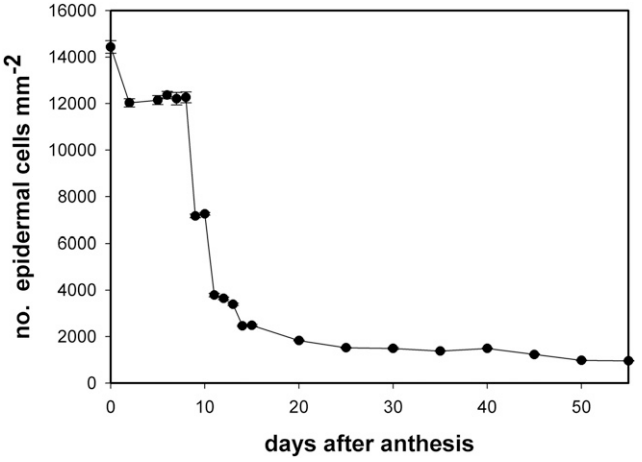

Figure 1. Number of epidermal cells per surface unit (mm^2) during Cascada fruit growth. Data are expressed as mean ± SE.

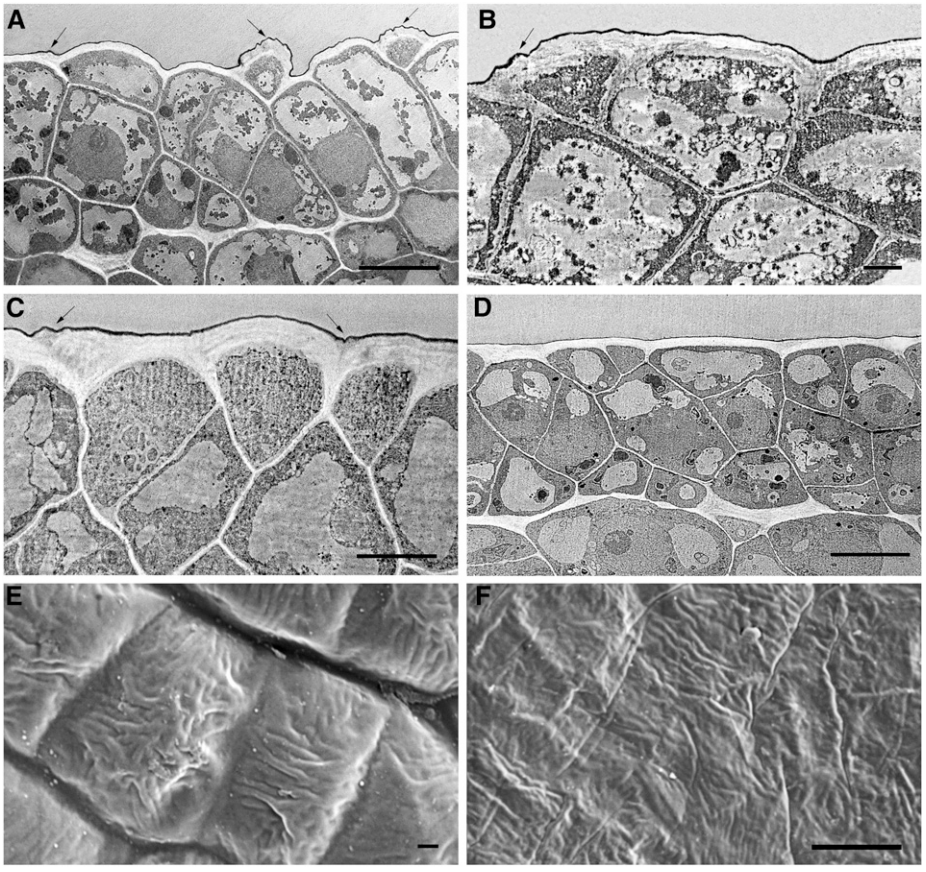

Figure 2. Electron microscopy pictures of the epidermis of Cascada fruits during the first 6 d of growth. TEM (A, B, C, D); Scanning electron microscopy (E, F). Ovary (A), bar 10 μm; 2 daa (B), bar 2 μm; 5 daa (C), bar 5 μm; 6 daa (D), bar 10 μm; ovary (E), bar 1 μm, 10 kV; 5 daa (F), bar 8 μm, 10 kV. Arrows indicate the presence of wrinkles.

to flatten and parenchyma tissue differentiation was initiated (Supplemental Fig. S1). However, the outermost 2 to 3 layers of cells still appeared disorganized and undifferentiated, showing different sizes and morphologies: cubical, triangular, or spherical (Fig. 2, C and D). Cuticle could be observed from the beginning as a very thin dark layer covering the outer walls of protodermal cells. The so-called cuticle ridges, which are commonly detected on surface images, could also be observed in the cross sections (see arrows in Fig. 2, A–C) and corresponded to OEW irregularities, not to local increases of cuticle material since cuticle thickness was not altered in these areas. At anthesis, these ridges were detected all over the surface (Fig. 2A) while later on they were restricted to the regions close to anticlinal walls (see arrows in Fig. 2, B and C). They slowly disappeared during the first 5 to 6 daa, and at 6 daa, the OEW surface was completely flattened (Fig. 2D). Fig. 2, E and F, shows scanning electron microscopy images of the tomato fruit surface where it could be observed that these ridges did not follow any orientation. The flattening of the surface during this period was also observed by scanning electron microscopy, with cells at anthesis showing a clear curvature and cells at 5 daa flattened. Differentiation of epidermal and hypodermal tissue started at 7 daa and was already finished at 8 daa (Fig. 3A). At this stage, an increase in cell size was also observed. Comparison of Fig. 3B (9 daa) and Fig. 3C (10 daa) showed a dramatic increase in cuticle deposition and thickness within a 1 d period. This was accompanied by the beginning of cuticle impregnation of epidermal radial walls initiating the so-called pegs (Fig. 3C). The increased cuticle deposition observed at 10 daa continued, and only 5 d later (15 daa) the thickness was doubled (Fig. 3D).

Figure 4 shows the average thickness of both the cuticle, i.e. cutinized cell wall, and the cell wall of tomato fruit from anthesis until 15 daa. Cuticle thickness slowly increased during the first 9 d, changing from 60 nm at anthesis to 480 nm at 9 daa, while at 10 daa it reached 5.3 μm. This sudden escalation in cuticle thickness was very noticeable and marked the beginning of a period of increasing cuticle thickness that reached 9.4 μm at 15 daa. The cell wall showed a similar pattern with a slow increase from anthesis to 9 daa followed by a higher rise in thickness during the 10 to 15 daa period. It is interesting to note that during the first 9 d period of growth, the thickness of the cell wall was significantly higher than that of the cuticle, while from 10 daa on this trend was reverted and cuticle thickness remained higher. Cell wall thickness was around 7-fold higher than cuticle's thickness during the first 6 d; later increase in cuticle thickness during 7 to 9 daa was not accompanied by a similar increase in the cell wall, and this fold-change was reduced to 2.5.

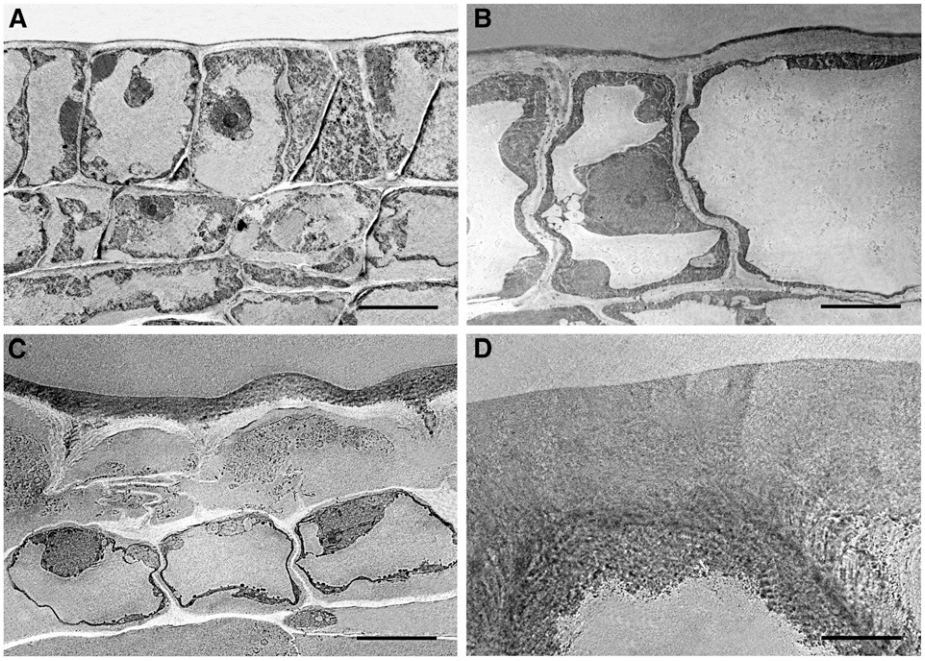

Figure 3. TEM pictures of epidermal cross sections of Cascada fruits. 8 daa (A), bar 10 μm; 9 daa (B), bar 5 μm; 10 daa (C), bar 10 μm; 15 daa (D), bar 5 μm.

Figure 5 shows high-magnification transmission electron microscopy (TEM) images of the cuticle during the cell division period. The cuticle was observed as a uniformly distributed and electron-dense thin layer at anthesis (Fig. 5A). At 2 daa, the inner side of the cuticle started showing a globular morphology (see arrows in Fig. 5B) albeit the cuticle still appeared as a very homogeneous electron-dense layer. This globular nature of the cuticle's inner side was more pronounced in later stages (Fig. 5, C–E) with the presence of nanoscopic, polydisperse (in size), and electron-dense particles, droplets, or vesicle-like particles randomly distributed in the cell-wall region in close contact with the cuticle. Thus, most part of the cuticle displayed a nonhomogeneous condition during the 5 to 9 daa period. At 10 daa (Fig. 5F), a reticulate region was observed on the upper half of the cuticle whereas the lower part still displayed a globular nature.

Epidermal Fine Structure during Cell Expansion

The cuticle and cell wall suffered few changes during cell expansion period. Cuticle thickness continued growing during this period and reached a maximum around 25 daa to later on decrease during the last stages of development and ripening (Fig. 6). Cell wall thickness also increased during this period until ripening. A plateau during the 15 to 40 daa was observed, with no significant changes in thickness, and the increase in thickness was resumed during ripening. Interestingly, around the breaker stage (45 daa), both cuticle and cell wall reached similar thicknesses and remained similar until red ripe. A transient increase at 50 daa was observed in both the cuticle and the cell wall.

Figure 7 shows TEM images of transverse epidermal sections. Cuticle pegs were well developed at 20 daa (Fig. 7A); deposition of cuticle material on the anticlinal and inner periclinal walls of the epidermis continued throughout this period until red ripe (Fig. 7, C and E). High magnification images of the cuticle during this period showed a homogenous electron-dense cuticle layer without distinction between layers with different osmiophilic behavior (Fig. 7, B, D, and F). The globular nature of the inner cuticle surface was lost during this period, despite cuticle deposition continuing throughout this period.

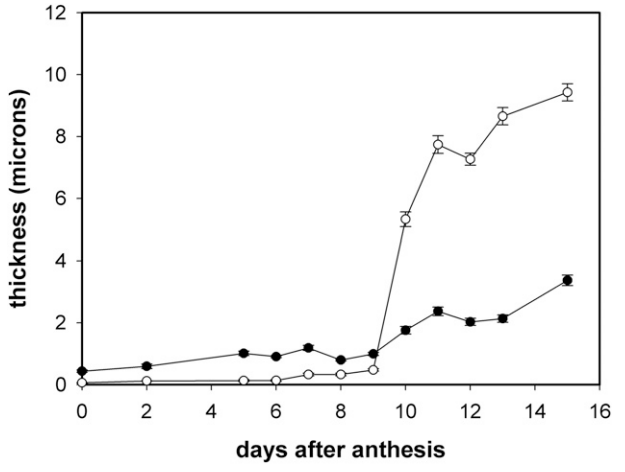

Figure 4. Evolution of cuticle and outer epidermal wall thickness during the early stages of fruit growth. Open circles, cuticle; solid circles, cell wall. Data are expressed as mean ± SE.

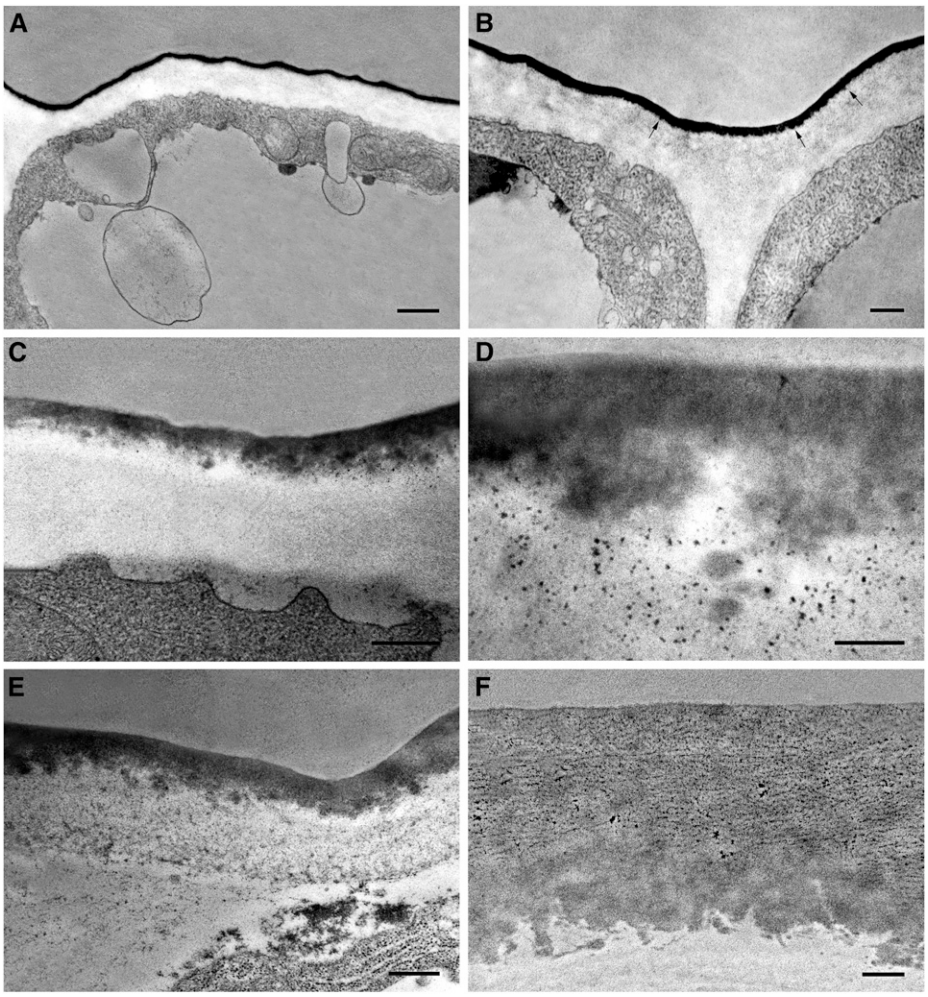

Figure 5. High magnification pictures of the epidermis of Cascada fruits during the cell division period. Ovary (A), bar 500 nm; 2 daa (B), bar 200 nm; 7 daa (C), bar 500 nm; 7 daa (D), bar 200 nm; 9 daa (E), bar 500 nm; 10 daa (F), bar 500 nm. Arrows indicate the location of globular structures.

Cell wall ultrastructure showed an amorphous, mostly electron-clear nature at early stages of development (Fig. 8A). At 5 daa, the cell wall started to show a reticulate nature (Fig. 8B). By 10 daa, this reticulate disappeared and an organized multilayered cell wall was detected (Fig. 8C). This cell wall structure of parallel layers of electron-dense and electron-clear material remained constant until ripening (Fig. 8, D–F).

Immunocytolocalization of Cell Wall Components to the OEW

Changes in cell wall composition were studied with antibodies against the main cell wall components: methyl-esterified and non-esterified pectin and cellulose. Table I shows changes in pectin and cellulose labeling density of the cell wall throughout during fruit development. The presence of non-methyl-esterified pectin was restricted to the early stages of development, from ovary to 7 daa (Fig. 9A), and was not detected during the rest of fruit development and ripening. On the contrary, methyl-esterified pectin was detected during the first stages of development (from ovary until 10 daa) (Fig. 9B) and later on during ripening with a lower density. During the period of cell expansion, esterified pectins were scarcely detected. Crystalline cellulose was detected in the cell wall during fruit growth but was absent during ripening (Fig. 9, C and D). Labeling was not restricted to any specific area of the cell wall but distributed along it. No labeling was detected within the cuticle.

DISCUSSION

According to the standard and prevalent nomenclature, the plant cuticle consists of two different layers: the cuticle proper as the outermost region that appears at early stages of development, and the underlying cuticular layer that appears later on in development by cutin impregnation of a portion of cell wall (Jeffree, 2006). Thus, the more electron-dense cuticle proper is mainly composed of cutin and is free of polysaccharides, whereas the cuticular layer also contains polysaccharides derived from the cell wall (Jeffree, 2006). In

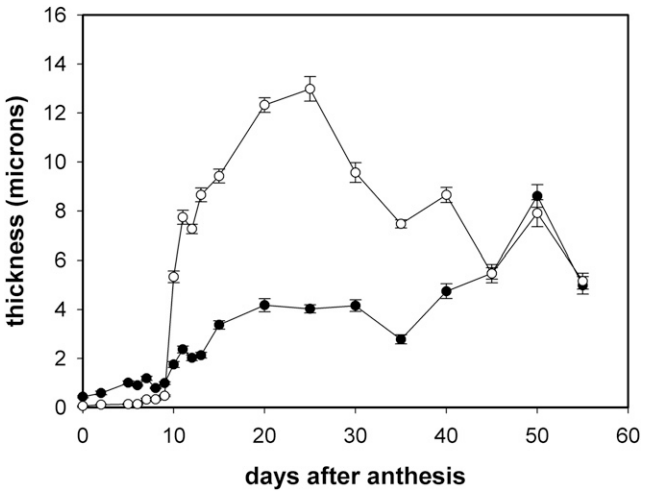

Figure 6. Changes in cuticle and outer epidermal wall thickness throughout fruit growth and ripening. Open circles, cuticle; solid circles, cell wall. Data are expressed as mean ± SE.

this work we have omitted this nomenclature for several reasons. Tomato fruit cuticle does not show regions of different electron-density but appears as a more or less homogeneous osmiophilic layer. Moreover, contrary to other species such as *Agave americana* L. and *Picea abies* (L.) H. Karst (Jeffree, 2006), no clear boundary between a fibril-rich and non-fibril region can be detected within the cuticle. In this sense, OEW localization of cell wall components with antibodies failed to identify their presence in the cuticle, most probably because its dominant lipid nature hindered epitope recognition. Epitope masking has been reported to hinder recognition of cell wall components (Marcus et al., 2008). Therefore, we only differentiate two regions in the OEW: the cuticle (or cutinized cell wall) and the cell wall (or non-cutinized cell wall), based on the presence or absence of osmiophilic material of lipid nature.

Tissue Differentiation

In the short period spanning between anthesis and 2 daa, fertilization had occurred and fruit set had been initiated. This was clearly observed from the significant change in fruit size (almost doubling) that happened during this period, plus the histological changes observed in cross sections. At 2 daa, parenchyma differentiation had started and cells had increased their size and initiated a layered arrangement. However, the first three layers, which correspond to the future epidermis and collenchyma, remained undifferentiated. Epidermis and collenchyma differentiation did not start until 7 daa, before the beginning of the cell expansion period. Despite organization of the epidermal layer and cell arrangement, which did not start until 7 daa, the most distinguishing feature of epidermal cells, a thick and cutinized OEW, was already present in the ovary.

Organs exhibit specific spatial and temporal patterns of growth (Anastasiou and Lenhard, 2007). This growth is a combination of two integrated processes, cell division and cell expansion. Whereas the first is mostly limited to early stages of development, cell expansion is responsible for most of an organ's growth and mainly occurs after cell division has ceased. In cherry tomatoes, transition between division and expansion occurs around 11 to 14 daa (Bertin et al., 2007; España et al., 2014). Several transcriptional factors involved in the regulation of cell division and expansion have been identified (Anastasiou and Lenhard, 2007). Recently, changes in cuticle mechanical properties were associated with the transition between cell division and expansion (España et al., 2014). Results reported here also showed a temporal correlation among changes in OEW morphological and biochemical traits and the transition between these two processes of organ growth. During cell division, the OEW was thin and mostly composed of non-cutinized cell wall rich in non-esterified and esterified pectin whereas the transition to cell enlargement was accompanied by a dramatic increase of the OEW's thickness due to cuticle accumulation, and pectin epitopes were barely detected in the remaining non-cutinized cell wall. Thus, during cell expansion the cuticle represented 60% to 75% of the OEW thickness. Fujino and Itoh (1998) also observed a significant increase in OEW thickness in pea stems between elongating and non-elongating cells. In this sense, cuticle thickness was 4-fold higher in elongating cells whereas cell wall only showed a 2.5-fold. Recently, it was reported how changes in the cutin/polysaccharide ratio present in the cuticle affected the strength required to achieve viscoelastic deformation, and thus growth (España et al., 2014). At the whole OEW level, it would be most interesting to investigate whether the dramatic change in thickness of the cuticle/cell-wall ratio observed during the transition between cell division and elongation plays a similar mechanical role.

The Discontinuous Construction of the Cutinized Cell Wall

At anthesis, fruit surface showed the presence of multiple wrinkles without any clear orientation that disappeared during the next 5 d of fruit growth. These cuticle folds have also been observed in *Vitis vinifera* L. fruits (Considine and Knox, 1979; Casado and Heredia, 2001) and in the leaves of apple (Bringe, 2007), *Aesculus hippocastanum* L. (Martin and Juniper, 1970), *Syringa vulgaris* L. (Holloway, 1971), and *Acer pseudoplatanus* L. (Wilson, 1984) among other species. However, their evolution has only been characterized in grape and apple fruits, with surface flattening observed during organ development (Casado and Heredia, 2001; Bringe, 2007). According to Rosenquist and Morrison (1988), these folds represent storage of cuticle material that spread out during the period of rapid growth. However, epidermal cross sections showed that these folds

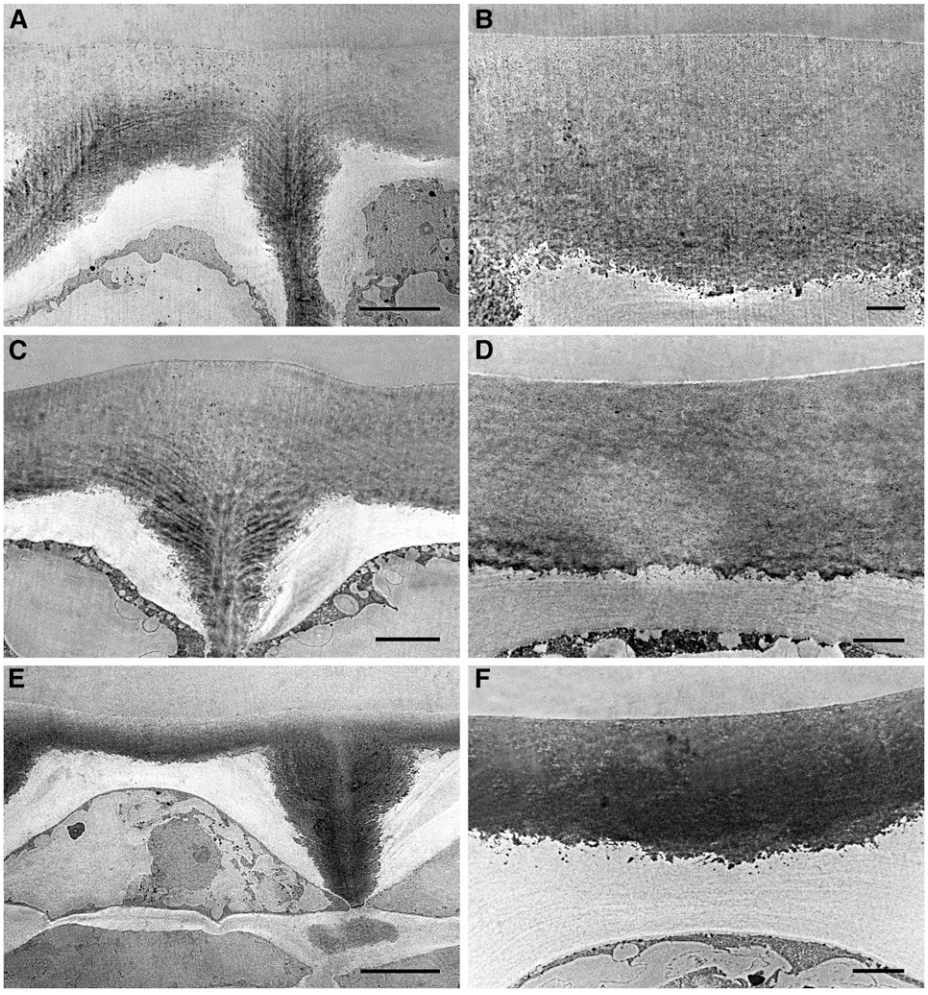

Figure 7. TEM pictures of epidermal cross sections of Cascada fruits during cell expansion and ripening. A, B, 20 daa, bar 10 μm (A) and 2 μm (B); C, D, 35 daa, bar 10 μm (C) and 2 μm (D); E, F, 55 daa, bar 10 μm (E) and 2 μm (F).

are not only composed of cuticle, but they represent an irregular cell-wall contour covered by a cuticle. The fact that these wrinkles began to disappear the moment fruit growth started, that epidermal surface was completely flat at 6 daa, when only 10% of fruit growth has occurred, and that they were already present prior to anthesis (Supplemental Fig. S2) suggests that these folds could play a different role, maybe related to the irregular protodermal surface present in the ovary. As Jeffree (1996) pointed out, the presence of folds increases surface area by a factor of 2 to 3. These wrinkles probably play a different role to those found on the surfaces of full developed petals (Jeffree, 2006) and referred to as ridges or nanoridges (Li-Beisson et al., 2009).

Changes associated with the beginning of fruit set were also detected at the cuticle level. At anthesis, the cuticle appeared as a very narrow but well-defined electron-dense layer. Two days later, the cuticle doubled its thickness, although it remained as a very thin layer with a globular and irregular inner surface visible. Until 9 daa, the cuticle moderately increased its thickness and the globular profile of its inner face in contact with the cell wall was increasingly manifest. Following the literature on cuticle ultrastructure, this thin layer present until 9 daa can be regarded as the procuticle (Jeffree, 2006). The procuticle is considered an early stage of cuticle development and it is believed to be composed of cutin only. According to Jeffree (2006), the procuticle is underlain by a superficial layer that behaves as a polyanion and is predominantly pectic in nature (Jeffree, 2006). The procuticle has been identified in only a few species (see references in Jeffree, 2006) and in this work, to our knowledge, is reported for the first time in tomato fruit. The variable shape, mostly of its inner side, and thickness of this procuticle (Fig. 5, C–E) is probably a consequence of the progressive molecular arrangement and assembly of cutin molecular domains that happens at an early growth stage. The globules in contact with the inner side of the procuticle were also observed as small osmiophilic droplets and globular-like particles along the underlying cell wall (Fig. 5, D and E). These globular-like particles, of varying size, seem to migrate thorough the wall matrix to the cuticle. This fact has been clearly observed by several authors and these particles have been considered

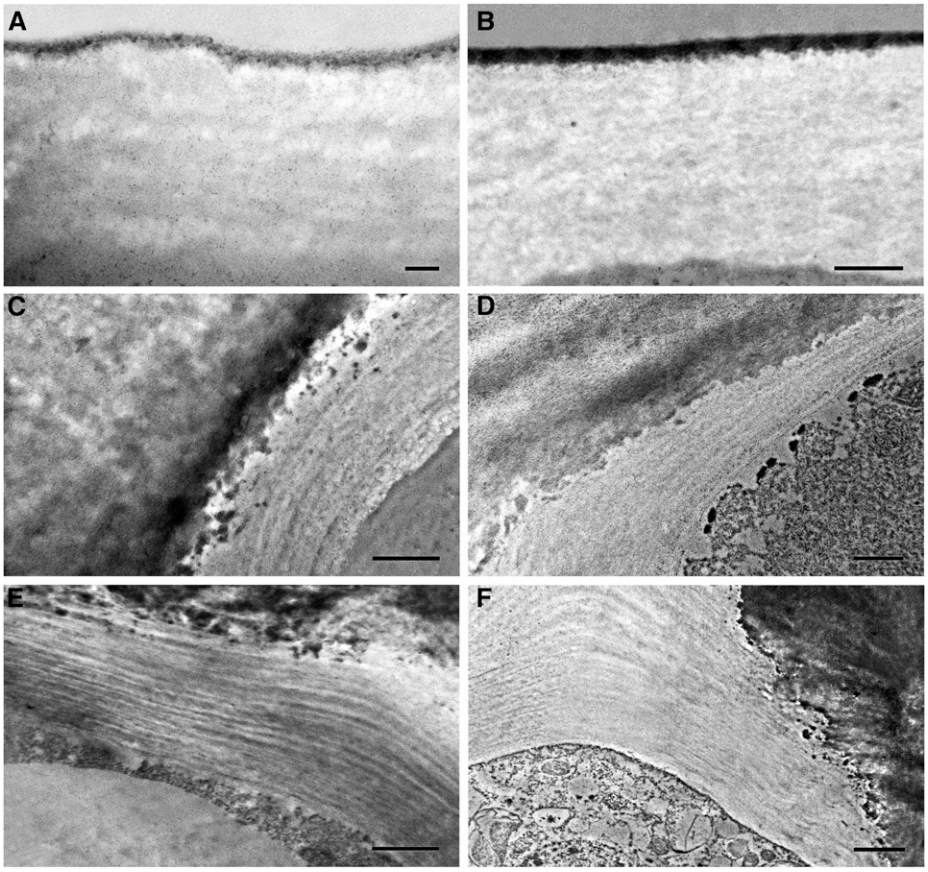

Figure 8. Cell wall ultrastructure of Cascada fruit epidermis. 2 daa (A), bar 0.2 μm; 5 daa (B), bar 0.5 μm; 10 daa (C), bar 1 μm; 14 daa (D), bar 1 μm; 30 daa (E), bar 1 μm; 50 daa (F), bar 2 μm.

procutin precursors (Frey-Wyssling and Mühlenthaler, 1965; Hallam, 1970; Heide-Jørgensen, 1978, 1991; Jeffree, 2006). In this study there were no clear indications of where this lipid material is synthetized or how it is transported to the surface of protodermal cells. Nevertheless, accumulation and fusion of the above-mentioned nanodroplets or nanoparticles at the outer part of epidermal plant cell wall has been suggested as a possible mechanism for early cutin or procuticle formation (Heredia-Guerrero et al., 2008; Domínguez et al., 2010; D'Angeli et al., 2013; Kwiatkowska et al., 2014). During the cell expansion period (from around 11 daa until red ripe), the cuticle showed few changes in appearance and fine structure. It could be said then that the main framework has already been constructed and the only observable changes during this period were further development of invaginations between neighboring epidermal cells and cuticle thickening most probably due to rearrangement of the lipid matrix, since the amount of isolated cutin did not change during this period (Domínguez et al., 2008).

Cuticle development showed two marked changes in thickness. During the first 9 d, cuticle thickness was within the nanometric scale, whereas at 10 daa, due to a sudden 11-fold increase, it reached the micrometric scale. This change in cuticle thickness agrees with the results previously reported for the same cultivar using selective dyes and conventional microscopy and was accompanied by a 4-fold increase in cuticle material (Domínguez et al., 2008). It is interesting to note that, although the thickness values herein obtained were similar to those reported by Domínguez et al. (2008), there is a significant discrepancy at 10 daa. Values reported here

Table I. *Pectin and cellulose labeling density during tomato fruit development*

Labeling density in the outer epidermal wall is expressed as the number of gold particles per μm^2.

Stage (daa)	Non-Esterified Pectin	Esterified Pectin	Crystalline Cellulose
Ovary	2.7 ± 0.4	3.9 ± 0.3	3.9 ± 0.4
2	2.7 ± 0.1	3.0 ± 0.4	1.3 ± 0.1
5	2.7 ± 0.7	4.1 ± 0.3	2.7 ± 0.3
7	2.9 ± 0.4	3.6 ± 0.2	3.1 ± 0.2
9	—	3.5 ± 0.3	3.2 ± 0.4
10	—	3.4 ± 0.2	3.7 ± 0.3
15	—	—	3.1 ± 0.3
20	—	—	4.5 ± 0.3
25	—	—	5.5 ± 0.5
35	—	—	5.5 ± 0.8
45	—	2.4 ± 0.1	—
55	—	2.2 ± 0.3	—

Data are presented as mean ± SE. Controls without primary antibodies showed label density < 0.3. daa, days after anthesis; (—), no labeling or very disperse gold particles.

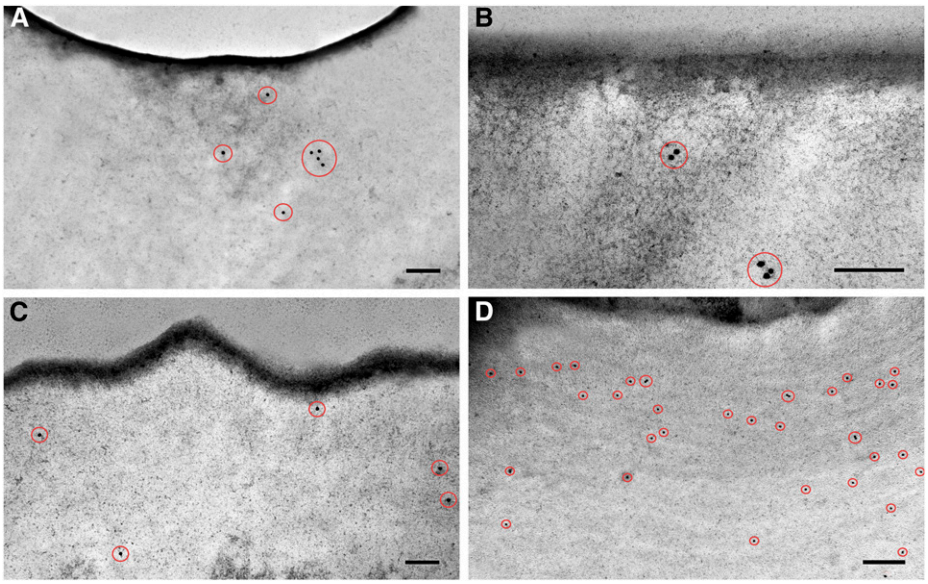

Figure 9. Immunolocalization of cell wall components in epidermal cross sections of Cascada fruits. 7 daa non-esterified pectin (A); 5 daa esterified pectin (B); ovary crystalline cellulose (C); 35 daa crystalline cellulose (D). Gold particles are encircled in red. Bars = 200 nm.

are higher probably because osmium is more sensitive to low quantities of lipid material than Sudan IV. Cuticle thickness continued rising until 25 daa, followed by a decrease during the ripening period. This decrease in thickness was not accompanied by a loss of cuticle material, which suggests a rearrangement of cuticle material during this period.

The Growing Non-Cutinized Cell Wall: a Complex and Heterogeneous Structure

The polysaccharide cell wall, which serves as a framework for cuticle deposition and development, is also a dynamic supramolecular structure in continuous change during growth. A significant increase in thickness was observed throughout development, although much lower than in the case of the cuticle. This change in thickness was more prominent during the cell division stage when the cell wall showed a 4-fold increase in a very short period of time. Later, this growth continued at a slower pace until 20 daa. From this period until the end of ripening, the cell wall did not modify its thickness except for a transient increase during ripening. Cell wall swelling is known to occur during fruit ripening in several species (Redgwell et al., 1997).

Most studies on cuticle development are not accompanied by an examination of the accompanying cell wall, with some exceptions (see Jeffree, 2006). On the other hand, only a few studies on cell wall changes during development are focused on the OEW, since it is considered a special cell wall, not comparable to other cell walls. Despite the significant number of studies on cell wall composition and analysis, isolation and further analysis of the OEW is not trivial. Microscopic analysis of the OEW of pea stems showed higher cellulose content than typical primary walls (Bret-Harte and Talbott, 1993). Isolation of the polysaccharide fraction of mature tomato fruit cuticles showed an equimolecular contribution of the three main components of cell wall:

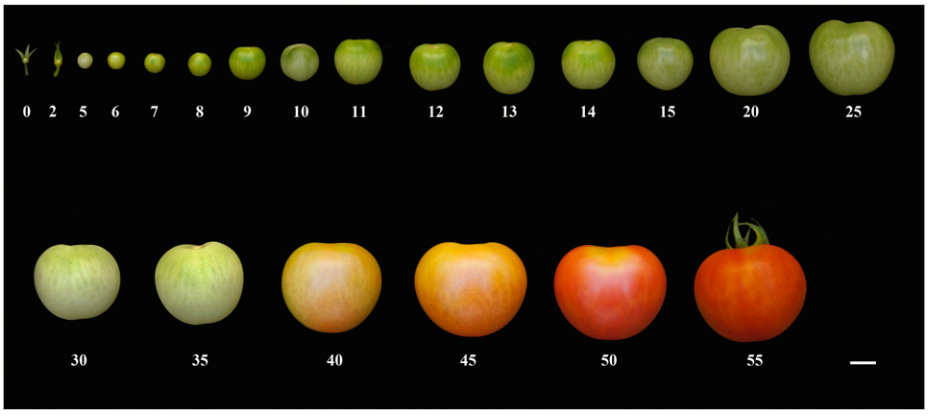

Figure 10. Photograph of Cascada fruits at the different stages of development studied in this work. Numbers indicate days after anthesis; 0 refers to anthesis. Bar = 1 cm.

cellulose, hemicellulose, and pectin (López-Casado et al., 2007). Recently, using enzyme-gold labeling, Guzmán et al. (2014) reported the identification and location of cellulose and pectin in isolated cuticles of *Eucalyptus* L'Hér., *Populus* L., and *Pyrus* L. leaves. In this work, results obtained by the use of antibodies against the ordered non-esterified pectin, the gelatinous esterified pectin, and crystalline cellulose allowed us to draw the following molecular scenario. Crystalline cellulose was present in the cell wall throughout development and only disappeared during ripening. This is in agreement with the biochemical analyses of tomato cell walls where the amount of cellulose remained constant during development and only decreased during ripening (Lunn et al., 2013). The presence of non-esterified pectin was constrained to early stages of development, the cell division period, and was not located during the expansion period. Esterified pectin, which forms part of the bulk of polysaccharides that compose the gel-like matrix of the walls (Burton et al., 2010), was found with a moderate and notable density during cell division, and later on during ripening. The scarce presence of methyl-esterified pectin during most of the cell expansion period could be due to a reduction of the molecules, but the possibility of epitope masking during this period should also be considered (Marcus et al., 2008).

Several studies point to a role of pectin methyl-esterification in cell wall expansion. Thus, immunocytochemical analyses of root cells showed that dividing cells contained lower levels of non-esterified pectins whereas no differences in esterified pectins were observed between dividing and non-dividing cells (Dolan et al., 1997). Similarly, elongating epidermal cells have less non-esterified pectin than non-elongating cells (Fujino and Itoh, 1998). Low pectin methyl-esterification has also been shown to decrease cell elongation in several cases (Derbyshire et al., 2007; Guénin et al., 2011), although the opposite behavior has also been reported (Pelletier et al., 2010). It has been suggested that local distribution of cell wall polysaccharides, mainly pectins, could also play an important role in cell wall physicochemical properties (Levesque-Tremblay et al., 2015). In this sense, a heterogeneous transversal distribution of esterified and non-esterified pectins in the OEW of flax and pea was found, with non-esterified pectins mainly located to the outer part of the OEW and esterified pectins more abundant in the inner part (Jauneau et al., 1997; Fujino and Itoh, 1998). Our results, however, did not show any distribution pattern for any of the cell wall polymers studied.

It is interesting to note the change in cell wall ultrastructure that appeared during the onset of cell expansion, with parallel multilayers disposed in a helicoidal form (Fig. 8). This arrangement agrees well with the construction of the OEW discussed by Kutschera (2008) and is composed of an ordered pattern with helicoidally organized layers of inextensible cellulose microfibrils. This pattern has been suggested to be the consequence of a well-organized self-assembly mechanism (Rey, 2010).

Many studies have been conducted to analyze the cell wall modifications that accompany fruit ripening (Brummell, 2006). In tomato, a decrease in cellulose and an increase in non-esterified pectin are observed during ripening (Roy et al., 1992; Steele et al., 1997; Lunn et al., 2013). However, these studies have been carried out in parenchyma cell walls but not in the OEW. Our results suggest a slightly different behavior in the OEW: a decrease in crystalline cellulose during ripening, and an increase in esterified pectins.

CONCLUSIONS

Results herein presented showed that the OEW is a highly dynamic structure that is significantly modified during the early stages of fruit growth. A deep interconnection and coordination between the two supramolecular structures that compose the OEW, i.e. the polyester cutin and cell wall polysaccharides, was observed. Further research will be necessary to investigate the molecular signals that trigger this synchronized development. In view of these results, the plant cuticle should be explained within the epidermis framework. In this sense, cuticle mutants would be an excellent material to study the interaction between the epidermis and the cuticle and could shed new light on the role of several cuticle genes. Given the significant role of the epidermis in organ development and fruit quality, these results will be valuable to create new commercial varieties with desired traits. Finally, this work (to our knowledge) shows for the first time the importance of the early stages of fruit development in cutin arrangement and deposition—a period of time that any proposed mechanism of cutin synthesis should take into careful consideration.

MATERIALS AND METHODS

Plant Material

Solanum lycopersicum L. Cascada plants were grown in a polyethylene greenhouse during spring. A random design of three blocks with 10 plants per block was employed. Experiments were conducted at the Estación Experimental La Mayora, Consejo Superior de Investigaciones Científicas, in Málaga, Spain. Tomato seedlings were grown in an insect-proof glass house, and plants were then transplanted to soil in a plastic house at the three-true-leaf-growth stage. The within-row and between-row spacing was 0.5 and 1.5 m, respectively. Plants were watered when necessary using a nutrient solution (Cánovas, 1995) and were supported by string and pruned to a single stem. The harvesting period lasted from early May until middle July. Flowers were labeled at anthesis and fruits collected at selected time points, from anthesis to red ripe (see Fig. 10). Fruit diameter was measured with a caliper from a minimum of 100 fruits (Supplemental Fig. S3).

Tissue Sectioning and Immunolabeling for TEM

Three fruits per developmental stage were harvested and small pericarp pieces of each fruit were cut and fixed overnight with 4% paraformaldehyde in 0.1 M phosphate buffer (pH 7.4), rinsed in the same buffer and postfixed in 1% OsO_4 in distilled water for 1 h. After dehydration in a graded ethanol-water series from 50 to 100%, the samples were embedded in LR White resin and polymerized in BEEM capsules for 48 h at 65°C. Ultrathin sections (around 50 nm thick) were cut with a Reichert Jung Ultracut ultra-microtome (Reichert

Technologies, Vienna, Austria) using a glass knife. Sections were placed onto nickel-Formvar-coated grids and examined in a JEOL JEM-1400 (Akishima, Tokyo, Japan) TEM at 80-kV acceleration voltage.

Prior to visualization, some samples were labeled with different antibodies to study cell wall structure. Sections were treated with 10% hydrogen peroxide for 15 min to remove osmium and washed in distilled water and in phosphate-buffered saline (PBS) buffer (0.01 M, pH 7.4) (Kwiatkowska et al., 2013). Samples were then blocked with small drops of PBS buffer containing 3% bovine serum albumin for 1 h at room temperature and later washed three times in PBS buffer. Rat monoclonal antibodies LM19 and LM20 (www.plantprobes.net) were employed to label non-esterified and methyl-esterified homogalacturonan domains of pectin, respectively. Sections were incubated in a 10-fold dilution of LM19 or LM20 in PBS buffer for 1.5 h. After a series of three washes in PBS buffer, grids were incubated in a 50-fold dilution of goat anti-mouse IgG coupled to 15 nm diameter colloidal gold particles (Aurion, Wageningen, The Netherlands) and incubated at room temperature for 1 h. His-tagged recombinant CBM3a (carbohydrate-binding module) protein (www.plantprobes.net) was employed to detect crystalline cellulose (Blake et al., 2006). Sections were incubated in a 100-fold dilution of CBM3a in PBS buffer with 0.1% bovine serum albumin for 1 h at room temperature. Samples were then incubated in a 100-fold dilution of mouse anti-His monoclonal antibody (Sigma-Aldrich, St. Louis, MO) in PBS buffer for 1.5 h. After three washes in PBS buffer, grids were incubated in the same secondary antibody as sections immunolabeled with LM19 and LM20. After a thorough wash in distilled water, all sections were stained with a 4% uranyl acetate solution for 15 min and later on carefully washed with distilled water. Controls without primary or secondary antibodies were also carried out.

Scanning Electron Microscopy and Epidermal Cell Number

Small pieces of pericarp from three biological samples at each stage of development were fixed in 2.5% glutaraldehyde in PBS buffer pH 7.2, and later on dehydrated in an ethanol series and their surfaces inspected with a scanning electron microscope (model no. JSM-840; JEOL). Five images from each biological sample were taken and the number of cells per surface area counted using ImageJ (Rasband, 1997–2014).

Statistics

Cuticle and cell wall thickness measurements were estimated from the cross-sectioned samples at each stage using an image capture analysis program (Visilog v. 6.3; Noesis, Crolles, France). It was assessed from the central region between pegs as this area remains almost constant and is not affected by cuticle invaginations. The density of labeling, i.e. the number of gold grains per unit area (μm^2), was estimated using the same program. Thirty micrographs were analyzed for each stage of development. Data are expressed as mean ± SE.

Supplemental Data

The following supplemental materials are available.

Supplemental Figure S1. TEM image of Cascada fruit pericarp at 2 daa. Bar = 10 μm.

Supplemental Figure S2. Scanning electron micrograph of Cascada ovary surface at 2 d before anthesis (dba). Bar = 5 μm.

Supplemental Figure S3. Cascada fruit diameter during development.

ACKNOWLEDGMENTS

We thank the Electron Microscopy Facility at the Universidad de Málaga for helpful assistance.

Received November 9, 2015; accepted December 8, 2015; published December 14, 2015.

LITERATURE CITED

Anastasiou E, Lenhard M (2007) Growing up to one's standard. Curr Opin Plant Biol **10:** 63–69

Baker EA, Bukovac MJ, Hunt GM (1982) Composition of tomato fruit cuticle as related to fruit growth and development. *In* DF Cutler, KL Alvin, CE Price, eds, The Plant Cuticle. Academic Press, London, UK, pp 33–44

Bargel H, Koch K, Cerman Z, Neinhuis C (2006) Structure–function relationships of the plant cuticle and cuticular waxes—a smart material? Funct Plant Biol **33:** 893–910

Becker T, Knoche M (2012) Deposition, strain, and microcracking of the cuticle in the developing 'Riesling' grape berries. Vitis **51:** 1–6

Beisson F, Li-Beisson Y, Pollard M (2012) Solving the puzzles of cutin and suberin polymer biosynthesis. Curr Opin Plant Biol **15:** 329–337

Bertin N, Lecomte A, Brunel B, Fishman S, Génard M (2007) A model describing cell polyploidization in tissues of growing fruit as related to cessation of cell proliferation. J Exp Bot **58:** 1903–1913

Blake AW, McCartney L, Flint JE, Bolam DN, Boraston AB, Gilbert HJ, Knox JP (2006) Understanding the biological rationale for the diversity of cellulose-directed carbohydrate-binding modules in prokaryotic enzymes. J Biol Chem **281:** 29321–29329

Bret-Harte MS, Talbott LD (1993) Changes in composition of the outer epidermal cell wall of pea stems during auxin-induced growth. Planta **190:** 369–378

Bringe K (2007) Surface Characteristics of *Malus domestica* Borkh. Leaves and Fruits as Influenced by Ontogenesis and Environmental Factors. Cuvillier Verlag, Göttingen, Germany

Brummell DA (2006) Cell wall disassembly in ripening fruit. Funct Plant Biol **33:** 103–119

Burton RA, Gidley MJ, Fincher GB (2010) Heterogeneity in the chemistry, structure and function of plant cell walls. Nat Chem Biol **6:** 724–732

Cánovas F (1995) Manejo del cultivo sin suelo. *In* F Nuez, ed, El Cultivo del Tomate. Mundi Prensa, Madrid, Spain, pp 227–254

Casado CG, Heredia A (2001) Ultrastructure of the cuticle during growth of the grape berry (*Vitis vinifera*). Physiol Plant **111:** 220–224

Considine JA, Knox RB (1979) Development and histochemistry of the cells, cell walls, and cuticle of the dermal system of fruit of the grape, *Vitis vinifera* L. Protoplasma **99:** 347–365

D'Angeli S, Falasca G, Matteucci M, Altamura MM (2013) Cold perception and gene expression differ in *Olea europaea* seed coat and embryo during drupe cold acclimation. New Phytol **197:** 123–138

Derbyshire P, McCann MC, Roberts K (2007) Restricted cell elongation in Arabidopsis hypocotyls is associated with a reduced average pectin esterification level. BMC Plant Biol **7:** 31

Dolan L, Linstead P, Roberts K (1997) Developmental regulation of pectic polysaccharides in the root meristem of Arabidopsis. J Exp Bot **48:** 713–720

Domínguez E, Heredia-Guerrero JA, Benítez JJ, Heredia A (2010) Self-assembly of supramolecular lipid nanoparticles in the formation of plant biopolyester cutin. Mol Biosyst **6:** 948–950

Domínguez E, Heredia-Guerrero JA, Heredia A (2011) The biophysical design of plant cuticles: an overview. New Phytol **189:** 938–949

Domínguez E, Heredia-Guerrero JA, Heredia A (2015) Plant cutin genesis: unanswered questions. Trends Plant Sci **20:** 551–558

Domínguez E, López-Casado G, Cuartero J, Heredia A (2008) Development of fruit cuticle in cherry tomato *(Solanum lycopersicum*). Funct Plant Biol **35:** 403–411

España L, Heredia-Guerrero JA, Segado P, Benítez JJ, Heredia A, Domínguez E (2014) Biomechanical properties of tomato fruit cuticle during development are modulated by changes in the relative amount of their components. New Phytol **202:** 790–802

Frey-Wyssling A, Mühlenthaler A (1965) Ultrastructural Plant Cytology. Elsevier, Amsterdam, The Netherlands

Fry SC (2004) Primary cell wall metabolism: tracking the careers of wall polymers in living plant cells. New Phytol **161:** 641–675

Fujino T, Itoh T (1998) Changes in pectin structure during epidermal cell elongation in pea (*Pisum sativum*) and its implications for cell wall architecture. Plant Cell Physiol **39:** 1315–1323

Girard AL, Mounet F, Lemaire-Chamley M, Gaillard C, Elmorjani K, Vivancos J, Runavot JL, Quemener B, Petit J, Germain V, Rothan C, Marion D, et al (2012) Tomato *GDSL1* is required for cutin deposition in the fruit cuticle. Plant Cell **24:** 3119–3134

Glover BJ (2000) Differentiation in plant epidermal cells. J Exp Bot **51:** 497–505

Guénin S, Mareck A, Rayon C, Lamour R, Assoumou Ndong Y, Domon JM, Sénéchal F, Fournet F, Jamet E, Canut H, Percoco G, Mouille G, et al (2011) Identification of pectin methylesterase 3 as a basic pectin methylesterase isoform involved in adventitious rooting in *Arabidopsis thaliana*. New Phytol **192:** 114–126

Guzmán P, Fernández V, García ML, Khayet M, Fernández A, Gil L (2014) Localization of polysaccharides in isolated and intact cuticles of eucalypt, poplar and pear leaves by enzyme-gold labelling. Plant Physiol Biochem **76:** 1–6

Hallam ND (1970) Leaf wax fine structure and ontogeny in *Eucalyptus* demonstrated by means of a specialized fixation technique. J Microsc **92:** 137–144

Heide-Jørgensen HS (1978) The xeromorphic leaves of *Hakea suaveolens* R. Br. II. Structure of epidermal cells, cuticle development and ectodesmata. Bot Tidsskr **72:** 227–244

Heide-Jørgensen HS (1991) Cuticle development and ultrastructure: evidence for a procuticle of high osmium affinity. Planta **183:** 511–519

Heredia A (2003) Biophysical and biochemical characteristics of cutin, a plant barrier biopolymer. Biochim Biophys Acta **1620:** 1–7

Heredia-Guerrero JA, Benítez JJ, Heredia A (2008) Self-assembled polyhydroxy fatty acids vesicles: a mechanism for plant cutin synthesis. BioEssays **30:** 273–277

Holloway PJ (1971) The chemical and physical characteristics of leaf surfaces. *In* TF Preece, CH Dickinson, eds, The Ecology of Leaf Surface Micro-Organisms. Academic Press, London, UK, pp 39–53

Holloway PJ (1982) Structure and histochemistry of plant cuticular membranes: an overview. *In* DF Cutler, KL Alvin, CE Price, eds, The Plant Cuticle. Academic Press, London, UK, pp 1–32

Hunt GM, Baker EA (1980) Phenolic constituents of tomato fruit cuticle. Phytochemistry **19:** 1415–1419

Jauneau A, Quentin M, Driouich A (1997) Micro-heterogeneity of pectins and calcium distribution in the epidermal and cortical parenchyma cell walls of flax hypocotyl. Protoplasma **198:** 9–19

Javelle M, Vernoud V, Rogowsky PM, Ingram GC (2011) Epidermis: the formation and functions of a fundamental plant tissue. New Phytol **189:** 17–39

Jeffree CE (1996) Structure and ontogeny of plant cuticles. *In* G Kerstiens, ed, Plant Cuticles: an Integrated Functional Approach. BIOS Scientific Publishers Ltd., Oxford, UK, pp 33–82

Jeffree CE (2006) The fine structure of the plant cuticle. *In* M Riederer, C Müller, eds, Biology of the Plant Cuticle. Blackwell Publishing, Oxford, UK, pp 11–125

Kutschera U (2008) The growing outer epidermal wall: design and physiological role of a composite structure. Ann Bot (Lond) **101:** 615–621

Kutschera U, Niklas KJ (2007) The epidermal-growth-control theory of stem elongation: an old and a new perspective. J Plant Physiol **164:** 1395–1409

Kwiatkowska M, Polit JT, Popłońska K, Stępiński D, Wojtczak A (2013) Immunogold method evidences that kinesin and myosin bind to and couple microtubules and actin filaments in lipotubuloids of *Ornithogalum umbellatum* ovary epidermis. Acta Physiol Plant **35:** 1967–1977

Kwiatkowska M, Wojtczak A, Popłońska K, Polit JT, Stępiński D, Domínguez E, Heredia A (2014) Cutinsomes and lipotubuloids appear to participate in cuticle formation in *Ornithogalum umbellatum* ovary epidermis: EM-immunogold research. Protoplasma **251:** 1151–1161

Lara I, Belge B, Goulao LF (2014) The fruit cuticle as a modulator of postharvest quality. Postharvest Biol Technol **87:** 103–112

Levesque-Tremblay G, Pelloux J, Braybrook SA, Müller K (2015) Tuning of pectin methylesterification: consequences for cell wall biomechanics and development. Planta **242:** 791–811

Li-Beisson Y, Pollard M, Sauveplane V, Pinot F, Ohlrogge J, Beisson F (2009) Nanoridges that characterize the surface morphology of flowers require the synthesis of cutin polyester. Proc Natl Acad Sci USA **106:** 22008–22013

López-Casado G, Matas AJ, Domínguez E, Cuartero J, Heredia A (2007) Biomechanics of isolated tomato (Solanum lycopersicum L.) fruit cuticles: the role of the cutin matrix and polysaccharides. J Exp Bot **58:** 3875–3883

Lunn D, Phan TD, Tucker GA, Lycett GW (2013) Cell wall composition of tomato fruit changes during development and inhibition of vesicle trafficking is associated with reduced pectin levels and reduced softening. Plant Physiol Biochem **66:** 91–97

Marcus SE, Verhertbruggen Y, Hervé C, Ordaz-Ortiz JJ, Farkas V, Pedersen HL, Willats WG, Knox JP (2008) Pectic homogalacturonan masks abundant sets of xyloglucan epitopes in plant cell walls. BMC Plant Biol **8:** 60

Martin JT, Juniper BE (1970) The Cuticles of Plants. Edward Arnold, Edinburgh, UK

Martin LBB, Rose JKC (2014) There's more than one way to skin a fruit: formation and functions of fruit cuticles. J Exp Bot **65:** 4639–4651

Pelletier S, Van Orden J, Wolf S, Vissenberg K, Delacourt J, Ndong YA, Pelloux J, Bischoff V, Urbain A, Mouille G, Lemonnier G, Renou JP, et al (2010) A role for pectin de-methylesterification in a developmentally regulated growth acceleration in dark-grown *Arabidopsis* hypocotyls. New Phytol **188:** 726–739

Pollard M, Beisson F, Li Y, Ohlrogge JB (2008) Building lipid barriers: biosynthesis of cutin and suberin. Trends Plant Sci **13:** 236–246

Rasband WS (1997–2014) ImageJ. U. S. National Institutes of Health, Bethesda, MD, http://imagej.nih.gov/ij/

Redgwell RJ, MacRae E, Hallett I, Fischer M, Perry J, Harker R (1997) In vivo and in vitro swelling of cell walls during fruit ripening. Planta **203:** 162–173

Rey AD (2010) Liquid crystal models of biological materials and processes. Soft Matter **6:** 3402–3429

Riederer M, Müller C (2006) Biology of the Plant Cuticle. Blackwell Publishing, Oxford, UK

Riederer M, Schönherr J (1988) Development of plant cuticles: fine structure and cutin composition of *Clivia miniata* Reg. leaves. Planta **174:** 127–138

Rosenquist JK, Morrison JC (1988) The development of the cuticle and epicuticular wax of the grape berry. Vitis **27:** 63–70

Roy S, Vian B, Roland JC (1992) Immunocytochemical study of the deesterification patterns during cell-wall autolysis in the ripening of cherry tomato. Plant Physiol Biochem **30:** 139–146

Samuels L, Kunst L, Jetter R (2008) Sealing plant surfaces: cuticular wax formation by epidermal cells. Annu Rev Plant Biol **59:** 683–707

Savaldi-Goldstein S, Peto C, Chory J (2007) The epidermis both drives and restricts plant shoot growth. Nature **446:** 199–202

Seymour GB, Østergaard L, Chapman NH, Knapp S, Martin C (2013) Fruit development and ripening. Annu Rev Plant Biol **64:** 219–241

Steele NM, McCann MC, Roberts K (1997) Pectin modification in cell walls of ripening tomatoes occurs in distinct domains. Plant Physiol **114:** 373–381

Thompson DS (2001) Extensiometric determination of the rheological properties of the epidermis of growing tomato fruit. J Exp Bot **52:** 1291–1301

Wilson J (1984) Microscopic features of wind damage to leaves of *Acer pseudoplatanus* L. Ann Bot (Lond) **53:** 73–82

Yeats TH, Martin LB, Viart HM, Isaacson T, He Y, Zhao L, Matas AJ, Buda GJ, Domozych DS, Clausen MH, Rose JKC (2012) The identification of cutin synthase: formation of the plant polyester cutin. Nat Chem Biol **8:** 609–611

Yeats TH, Rose JKC (2013) The formation and function of plant cuticles. Plant Physiol **163:** 5–20